EXTENDED ROTATION CURVES OF HIGH-LUMINOSITY SPIRAL GALAXIES. IV. SYSTEMATIC DYNAMICAL PROPERTIES, Sa→Sc

VERA C. RUBIN,*† W. KENT FORD, JR.,* AND NORBERT THONNARD
Department of Terrestrial Magnetism, Carnegie Institution of Washington
Received 1978 June 7; accepted 1978 July 18

ABSTRACT

For a sample of 10 high-luminosity spiral galaxies, Sa through Sc, we have obtained accurate rotation curves which extend to about 80% of the de Vaucouleurs radii. For this sample: (1) All rotation curves are approximately flat, to distances as great as $r = 50$ kpc. Secondary velocity undulations indicate rotational velocities lower by about 20 km s^{-1} on the inner edges than on the outer edges of spiral features. (2) $V_{\max}$ is correlated with Hubble type, and total mass M is a function of both $V_{\max}$ and radius. At equal radii, $M(\text{Sa}) > M(\text{Sc})$. Hence, surface mass density decreases systematically along the Hubble sequence. (3) $V_{\max}$ is not correlated with luminosity or with radius. Galaxies with similar $V_{\max}$ have radii and luminosities which differ by factors of 2 and 3. This implies a large intrinsic scatter in the Tully-Fisher relation. (4) Masses are a few times $10^{11} M_\odot$ out to the de Vaucouleurs radius, and some masses approach $10^{12} M_\odot$ out to the Holmberg radius. M/L_B ratios are low, near 3.5. There is a weak suggestion that M/L_B is higher for early-type galaxies. While this is contrary to the accepted result of Roberts, masses for early-type galaxies are systematically low in his sample, due to an extrapolation procedure based on falling rotation curves.

Subject headings: galaxies: individual — galaxies: internal motions — galaxies: structure

I. INTRODUCTION

In the 50 years since Hubble (1926) introduced his classification sequence for galaxies, few systematic observational programs have attempted to study dynamical properties of galaxies as a function of Hubble type (HT). The constraints have been principally instrumental. Optical rotation curves (e.g., Burbidge and Burbidge 1975) have furnished valuable dynamical information, but generally only for the inner regions of late-type spirals. Neutral hydrogen observations have revealed integral properties of gas-rich systems (Roberts 1975), but with limited spatial resolution.

Available optical instrumentation now permits the detection of emission across a very large portion of the disks of spirals, well beyond the "turnover point" in the rotation curves. We have initiated a program to obtain spectra of spiral galaxies at high velocity resolution and at a large spatial scale, in order to study their properties as a function of HT. We now have velocities for 10 spirals, Sa through Sc, of high intrinsic luminosity. The galaxies, chosen with extreme care, have: angular diameters near 3′ or 4′ to match the KPNO/CTIO spectrograph slit lengths; high inclination so that uncertainties in inclinations produce little effect on rotational velocities and hence masses; high luminosity

as indicated by the widths of their 21 cm profiles (if available); and large linear diameters. Two of the galaxies, NGC 4378 and NGC 7217, were studied originally for other reasons. These, plus NGC 3672, have been discussed separately (NGC 3672, Rubin, Thonnard, and Ford 1977 [Paper I]; NGC 4378, Rubin et al. 1978 [Paper II]; NGC 7217, Peterson et al. 1978 [Paper III]). Distances are determined from the corrected velocities, and we adopt $H = 50$ km s^{-1} Mpc^{-1} throughout.

II. THE ROTATION CURVES

Optical spectra were obtained with the Kitt Peak and Cerro Tololo 4 m spectrographs plus Carnegie image tube, usually at 25 Å mm^{-1}. Errors in the rotational velocities (measuring errors plus projection uncertainties) are generally less than ± 8 km s^{-1} per point. Reproductions of eight spectra are shown in Figure 1 (Plate L3) (Papers II and III show the other two). Many striking features can be observed directly from the spectra. (1) *All rotation curves are approximately flat*, with only a slight rise or fall following the initial steep gradient. (2) Secondary velocity undulations occur at positions of spiral features. Rotational velocities are ~ 20 km s^{-1} lower on the inner edges of the arms than on the outer edges. This is especially noticeable in NGC 2998, whose velocities are plotted in Figure 2. While this confirms a prediction of the density wave theory, velocity gradients will exist also in any gravitational model with a mass concentration in the arms. (3) Nuclear emission is often strong, often exhibits a large velocity gradient, and often remains intense several kiloparsecs beyond the nucleus. There follows
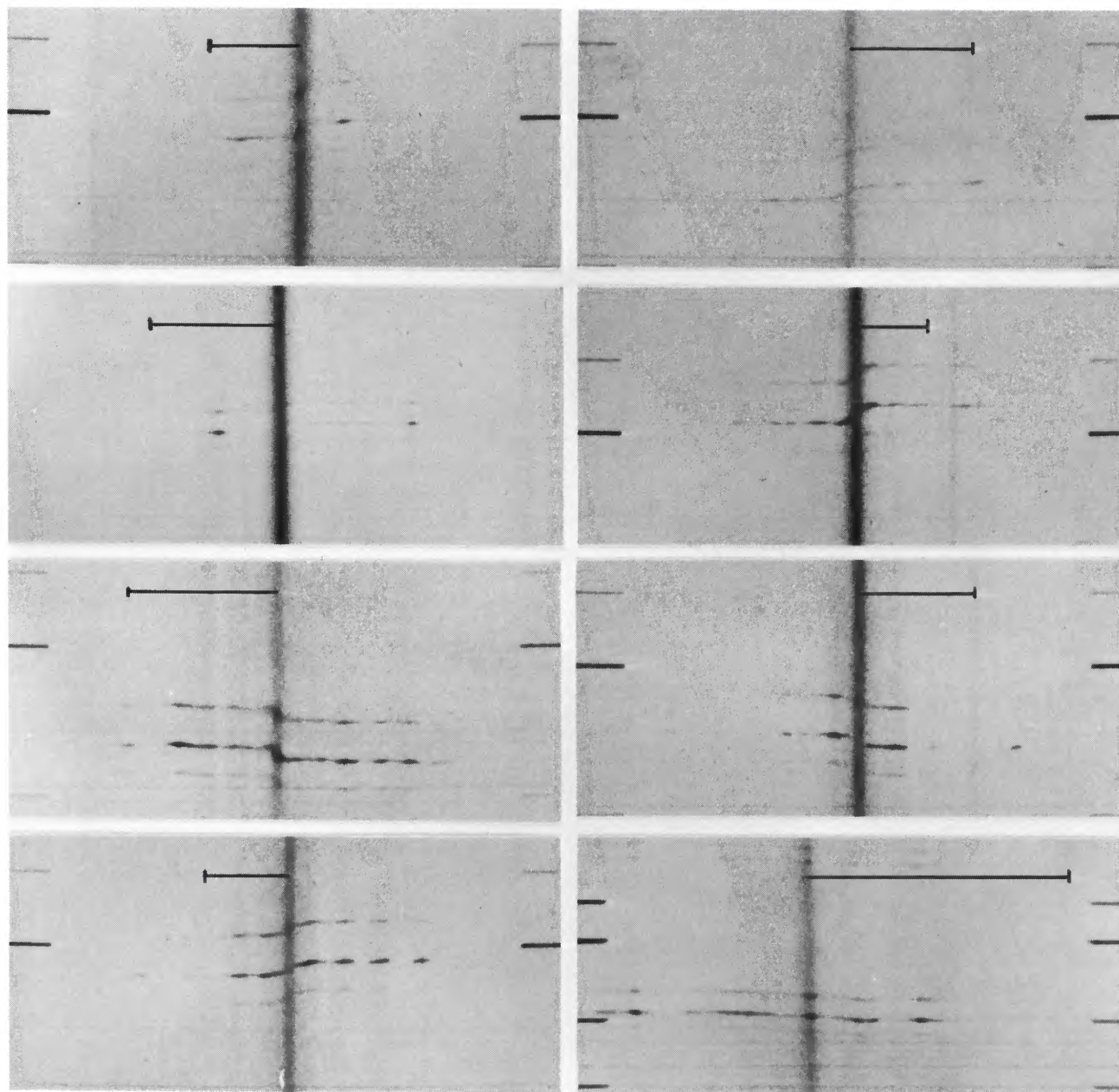
FIG. 1.—Hα region major axis spectra for galaxies of different Hubble types, taken with the 4 m RC spectrograph plus Carnegie image tube plus preflashed IIIa-J plate. Plates are (*) H₂ treated, 26 Å mm⁻¹, KPNO; or (†) N₂ baked, 52 Å mm⁻¹, CTIO. For all spectra, scale perpendicular to the dispersion is 24″ mm⁻¹, and transfer optics are f/2. (a)*NGC 2590, Sb, exposure 120 minutes. (b)*NGC 1620, Sbc, exposure 129 minutes. (c)†NGC 3145, Sbc I, exposure 90 minutes. (d)*NGC 801, Sbc–Sc, exposure 150 minutes. (e)*NGC 7541, Sbc–Sc, exposure 114 minutes. (f)*NGC 7664, Sbc–Sc, exposure 119 minutes. (g)*NGC 2998, Sc I, exposure 200 minutes. (h)†NGC 3672, Sc I–II, exposure 120 minutes. On each spectrum, Hα is strongest emission line; [N II] λ6583 is at longer λ (up on print). Vertical stripe is continuum from stars in nucleus. Solid horizontal line on each spectrum indicates 20 kpc in plane of galaxy. Linear extent of spectra varies from a radius of r = 17.4 kpc (NGC 2590) to r = 49 kpc (NGC 801). Note that velocity is often not constant across emission regions (spiral features) but is lower at inner edge and higher at outer edge, especially apparent in NGC 2998. The letters (a) and (b) refer to the upper left and upper right, respectively.

RUBIN et al. (see page L107)

a region of weaker emission with a shallow velocity minimum. Beyond this minimum the emission increases in intensity, with a corresponding velocity increase where the first spiral feature is encountered. (4) Star formation is proceeding vigorously over great distances in a single galaxy. In NGC 801, emission extends to a radius of 49 kpc. (5) Nuclear spectra come in a wide variety; emission lines can be narrow with a large velocity gradient (NGC 801), or broad, with the entire gradient within the nucleus (NGC 7541).

Parameters for these galaxies discussed are listed in Table 1. Classifications come from de Vaucouleurs, de Vaucouleurs, and Corwin (1975) (hereafter RC2) and/or Sandage (1978). Three galaxies not listed in

TABLE 1

DATA FOR PROGRAM GALAXIES

NGC (1)	Hubble Class (2)	Source (3)	HELIOCENTRIC VELOCITY Opt. (km s⁻¹) (4)	21 cm (km s⁻¹) (5)	V_0 Opt. (km s⁻¹) (6)	Distance (Mpc) (7)	i (degrees) (8)	Radius r_{dev} (kpc) (9)	Nuclear Distance of Last Velocity (kpc) (10)	Fraction r_{dev} Observed (11)	Rotation Curve at Large r (12)
4378..	Sa I	deV;S	2540±12	2536	2428	48.6	35	23.4	22.0	0.94	Falling
4594..	Sa	deV	1076±10		911	18.2	84	23.6	15.	0.64	Rising
7217..	Sb–Sab III	deV;S	955±6	954±10	1236	24.7	35	13.8	11.0	0.80	Falling
2590..	Sb	N	4990±25	4992±20	4793	95.9	75	34.8	17.4	0.50	Rising
1620..	Sbc	deV	3496±10	3509±8	3424	68.5	70	30.8	21.9	0.71	Rising
3145..	Sbc I	deV;S	3650±15	3648±20	3414	68.3	61	30.8	25.3	0.82	Flat
801...	Sbc–Sc	N	5763±10	5764±20	5948	119.	86	57.1	49.1	0.86	Flat or rising
7541..	Sbc–Sc III	deV;S	2685±10	2665:	2873	57.5	72	28.6	23.2	0.81	Rising
7664..	Sbc–Sc	N	3464±10	3481±15	3709	74.2	58	35.6	28.1	0.79	Flat or rising
2998..	Sc I	deV;S	4767±10	4777±5	4781	95.6	62	39.1	34.0	0.87	Flat
3672..	Sc I–II	deV;S	1857±10	1867±10	1655	33.1	70	19.8	17.6	0.89	Flat

NGC (1)	Hubble Class (2)	V_{max} Opt. (km s⁻¹) (13)	V_{max} 21 cm (km s⁻¹) (14)	Disk Mass to Last Velocity ($10^{11} M_\odot$) (15)	Mass to r_{dev} ($10^{11} M_\odot$) (16)	$\int SdV$ (Jy km s⁻¹) (17)	H I ($10^{10} M_\odot$) (18)	H I/ $M(r_{dev})$ (19)	m_B (mag) (20)	$L_B{}^{b, i}$ ($10^{10} L_\odot$) (21)	$M(r_{dev})/$ $L_B{}^{b, i}$ (22)
4378..	Sa I	320	323	3.05	3.24/3.89	6.6	0.37	0.01	12.28 S	4.53±0.4	8.6±2
4594..	Sa	344		2.8							>5
7217..	Sb–Sab III	290	313	1.13	1.41/1.55	11.7	0.17	0.01	11.08 S	4.41±0.4	3.5±1
2590..	Sb	262	251	1.74	4.11/4.52	18.3	8.1	0.18	13.4 P	10.5±2	4.3±2
1620..	Sbc	248	231	1.95	2.96	27.7	4.7	0.16	12.62 P	9.20±2	3.2±1
3145..	Sbc I	251	273	2.55	3.11	37.7	4.1	0.13	12.35 S	10.5±1	3.0±1
801...	Sbc–Sc	248	224	3.73	4.40	15.8	11.	0.25	13.1 Z	23.8±9	1.8±2
7541..	Sbc–Sc III	238	236	1.92	2.46				12.45 S	7.05±0.7	3.5±1
7664..	Sbc–Sc	208	204	1.77	2.36	29.7	4.0	0.17	12.9 Z	7.38±3	3.2±1
2998..	Sc I	211	213	2.38	2.74	25.1	5.4	0.20	12.65 S	14.9±1.4	1.8±1
3672..	Sc I–II	208	223	1.07	1.22	66.3	2.7	0.22	11.66 S	4.45±0.4	2.7±1

NOTES TO TABLE 1

Col. (3).—N, Nilson 1973. S, Sandage 1978. deV, de Vaucouleurs *et al.* 1976.

Col. (5).—Thonnard *et al.* 1978 except: NGC 4378, Krumm and Salpeter 1976; NGC 7217, Paper III; NGC 7451, Shostak 1978, contaminated by companion, not included in optical–21 cm comparison.

Col. (6).—$V_0 = V_H + 300 \sin l \cos b$.

Col. (7).—Distance $= V_0/H$; $H = 50$ km s⁻¹ Mpc⁻¹.

Col. (8).—$\cos^2 i = [1.042 \, b^2/a^2 - 0.042]$; b/a from RC2 or Nilson 1973.

Col. (9).—Radius to 25 mag arcsec⁻² from de Vaucouleurs *et al.* 1976 or Nilson 1973.

Col. (13).—V_{max} from smooth rotation curve.

Col. (14).—$\Delta V/2 \sin i$; ΔV read at 25% of mean flux, corrected for filter width; see n. (5).

Col. (15).—Factor of 1.1 (Brandt 1960) included.

Col. (16).—/Mass × 1.2 (Sa). /Mass × 1.1 (Sab, Sb). $\epsilon_M = \pm 25\%$; except NGC 2590, $\epsilon_M = 50\%$.

Col. (17).—See n. (5).

Col. (18).—Corrected for optical depth effects at 21 cm after Roberts 1975.

Col. (19).—See n. (18).

Col. (20).—P, Peterson unpublished; $\sigma_m = \pm 0.4$ mag. S, Sandage 1978; $\sigma_m = \pm 0.1$ mag. Z, Zwicky *et al.* 1961–68, corrected by $\Delta m = -0.4$ mag. Correction established by 4 galaxies in common with Sandage 1978, $\sigma_m = \pm 0.4$ mag.

Col. (21).—Corrected for: $A_b = 0.13$ (csc $b - 1$); $A_i = 0.8 \log a/b$ (RC 2); σ_L comes from σ_m (n. 20).

Col. (22).—Error estimate from ϵ_M and σ_L.

NOTE.—All data for NGC 4594 are from Schweizer 1978.

RC2 have Nilson (1973) classifications. Sources for other data and corrections applied are indicated in the notes. Differences between the optical and the 21 cm velocities are small: $\langle V_{21} - V_{opt}\rangle = 5$ km s^{-1}. However, the mean velocity difference for four galaxies with velocities in RC2 is (ours−catalog) $= 77$ km s^{-1}. Velocity errors this large still permeate the best available catalogs. Columns (9), (10), and (11) give the galaxy
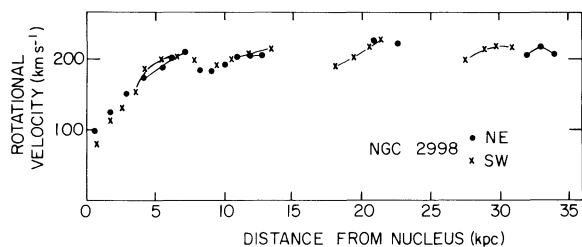

FIG. 2.—Rotational velocities in NGC 2998, as a function of distance from nucleus. Velocities for strongest emission regions are connected with lines. Note fairly good velocity agreement between velocities from NE and SW major axes, and positive velocity gradient across each arm.

radius (25 mag arcsec^{-2}; RC2), the radius of the last measured velocity, and the ratio of the two. In the mean, our velocities extend over 80% of the galaxy radius. V_{max}, the peak velocity of the optical rotation curve (in the plane of the galaxy), is listed in column (13). Data for NGC 4594 obtained by Schweizer (1978) with the same CTIO equipment are also included.

Rotation curves are plotted in Figures 3 and 4. The general flatness of the curves, and the pronounced increase in V_{max} with earlier HT, are notable. A plot of V_{max} versus HT, Figure 5, shows this tight correlation. A correlation between V_{max} and HT found earlier by Brosche (1971) lies about 50 km s^{-1} below that indicated in Figure 5, and is defined principally from galaxies with types later than Sbc. The correlation indicated in Figure 5 may represent an upper envelope defined by high-luminosity galaxies.

III. MASSES AND MASS-TO-LIGHT RATIOS

Masses and mass distributions have been determined from the rotation curves by two procedures: (1) disk-modeled galaxies, which give lower limits, and (2)
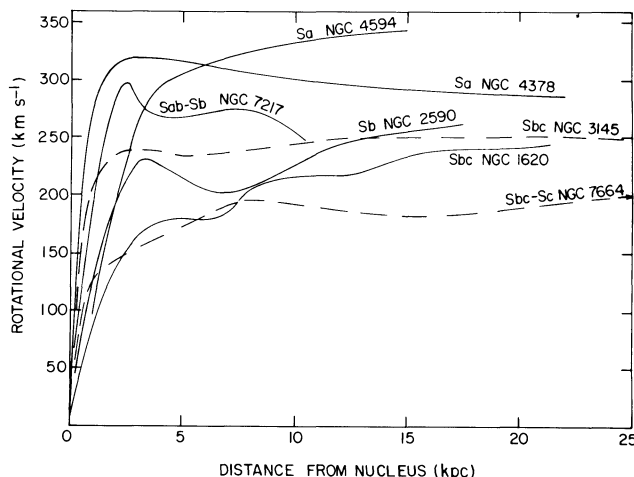

FIG. 3.—Rotational velocities for seven galaxies, as a function of distance from nucleus. Curves have been smoothed to remove velocity undulations across arms and small differences between major-axis velocities on each side of nucleus. Early-type galaxies consistently have higher peak velocities than later types.
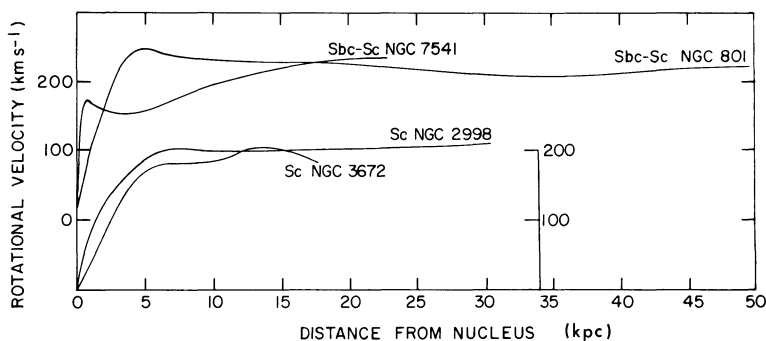

FIG. 4.—Rotation curves for two pairs of galaxies, which illustrate the lack of Tully-Fisher relation. NGC 7541 and NGC 801, both Sbc-Sc, have V_{max} values of 238 and 248 km s^{-1}. However, their luminosities (7.05 ± 0.7 and 23.8 ± 9 × 10^{10} $L_{\odot}$) and radii (23.2 and 49.1 kpc) differ by factors of 3 and 2. Similarly, the Sc galaxies NGC 2998 and NGC 3672 have V_{max} of 211 and 208 km s^{-1}, but luminosities 14.9 ± 1.4; 4.45 ± 0.4 × 10^{10} $L_{\odot}$ and radii 34.0 and 17.6 kpc.
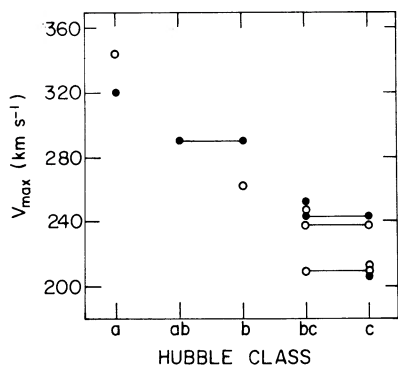
FIG. 5.—Maximum rotational velocity, in the plane of the galaxy, as a function of Hubble type. Galaxies with two classifications are entered twice with a connecting line. Open circles denote values of V_{max} which come from the last measured velocity (i.e., rising rotation curve).

spherical galaxies, which give upper limits to the masses. Both models are parameter independent. For the thin disk approximation (Kuz'min 1952), increased by 1.1 (Brandt 1960), integral masses as a function of radius (mass within a disk of radius r) are shown in Figure 6. The linear increase of mass with r is a consequence of the flat rotation curve: $M(r) = (2/G\pi) V^2(r)r$ for disk models, and V^2 is approximately constant. Because total mass varies both with r and V^2, and V is correlated with HT (Figure 5), total mass is a function of HT and of radius. While early-type galaxies have steeper mass gradients, dM/dr, large late-type galaxies (NGC 801, Figure 6) will have larger total masses than small early-type (NGC 4378). The *surface mass density decreases systematically along the Hubble sequence.*

The mass calculated to the last observed velocity, and the mass extrapolated to the RC2 radius, are listed in columns (15) and (16) of Table 1. If we had chosen to determine the masses from disk-plus-bulge models, then these masses would have been increased by about 1.2 (Sa) and 1.1 (Sab) times over the disk-molded masses. These refinements are included in column (16) and are discussed in Papers II and III. Masses to the RC2 radii lie in the range $1.2 < M(r_{deV}) < 4.5 \times 10^{11} M_{\odot}$; random errors should not exceed 25%. The expression $M(r_{deV}) = 1.5 \times 10^5 V^2 r$ (V in km s^{-1}, r in kpc) reproduces all 11 masses to within 20%, and seven of them to within 10%. Total masses calculated from integrated 21 cm profiles (Roberts 1975) are in good agreement with those calculated from the detailed optical rotation curves, but are about 20% smaller, due to the falling rotation curves adopted in the 21 cm models (Roberts 1969). If the exponent in the adopted Brandt (1960) curve is changed from 3 to 2, the 21 cm masses will agree with the disk-modeled masses determined from optical rotation curves.

For galaxies modeled as spheres, $M(r) = G^{-1}V^2 r$, or $\frac{1}{2}\pi$ (1/1.1) times that used above. The integrated mass out to any r is about 40% larger than the mass determined from the same rotation curve for a disk model.

For spherical models, and flat rotation curves, $M_{sph} = 2.1 \times 10^5 V^2 r$ is a good approximation to the mass distribution. For our sample, spherical models give $2 < M(r_{deV}) < 7 \times 10^{11} M_{\odot}$; out to their Holmberg radii (26.5 mag arcsec^{-2}), masses for some must approach $10^{12} M_{\odot}$. However, both disk and spherical mass distributions can reproduce the observed rotation curves.

By choosing to observe galaxies of high inclinations, we have maximized the accuracy of the rotational velocities and masses, but the uncertain internal extinction corrections pose a problem for the total magnitudes. The calculated blue luminosities (following RC2) and mass-to-blue-luminosity ratios are tabulated in columns (21) and (22). To the limits of the RC2 radii, integrated mass-to-luminosity ratios, M/L_B, are consistently small for this sample of high-luminosity spirals, near 3.5 for disk mass models, and about 5 for spherical mass models. Uncertainties in M/L_B are of the order of 1 or 2 in solar units, excluding systematic effects due to the choice of models and corrections applied.

There is a weak suggestion that M/L is higher for the earlier HT (col. [22]) a result in conflict with the widely quoted result (Roberts 1969) that M/L ratios are constant across the Hubble spiral sequence. However, five of the eight early-type galaxies in Robert's study had no 21 cm detection, so total masses come from limited optical measures, with extrapolation based on falling rotation curves. Hence, the masses for these early-type galaxies are too low by factors of from 2.5 to 5. Thus the earlier conclusions is probably not valid.

Previous correlations (Holmberg 1964) between high M/L and early HT have been questioned because of the procedure for obtaining masses (Sandage, Freeman, and
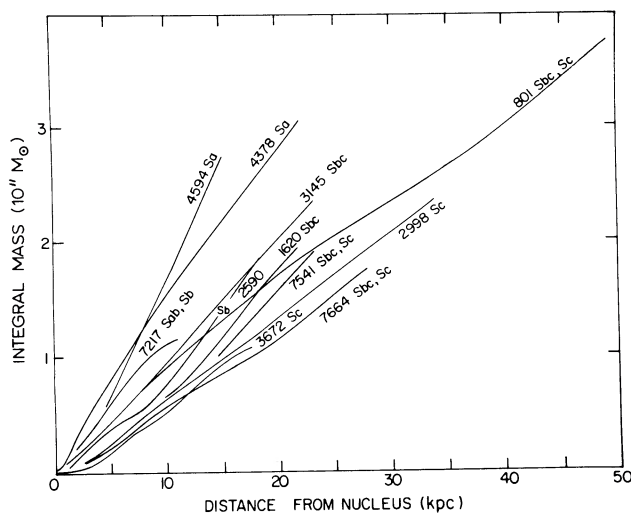

FIG. 6.—Integral mass within disk of radius r, as a function of r, for 11 galaxies, Sa through Sc, out to last measured velocity. Scale gives mass for disk models; masses for spherical galaxies are 1.4 times larger. Linear increase of mass with radius is a consequence of flat rotation curves. Mass gradient, dM/dr, is greater for early types, but total mass is a function both of V^2 and r. Surface mass density decreases systematically with Hubble type.

Stokes 1970). A correlation of M/L with HT might be expected from flat rotation curves ($M \propto V^2 r$), at least for galaxies of approximately equal radii, because of the relation between HT and V, and the tight correlation between luminosity and radius ($L \propto r^{2.4}$, Holmberg 1975). We prefer to keep an open mind on the question of whether M/L varies across the Hubble spiral sequence. At least some early-type galaxies have high M/L ratios.

IV. 21 CENTIMETER PROPERTIES

The 21 cm integrated flux densities, the hydrogen masses, and the hydrogen-mass–to–total-mass ratios are listed in columns (17), (18), and (19). H I constitutes 1% of the mass for our single Sa and Sab galaxies, but about 20% of the mass for the Sb and Sc galaxies.

From the 21 cm profile width, ΔV, we determine the peak velocity of the rotation curve, $V_{\max} = \Delta V/(2 \sin i)$ (col. [14]). This value is in good agreement with $V_{\max}$ (optical), found from the (resolved) optical rotation curve. The mean difference, $\langle V_{\max}$ (opt) $- V_{\max}$ (21 cm)$\rangle$, is 1 ± 6 km s^{-1}. A major surprise is the lack of a correlation of $V_{\max}$ (optical or 21 cm) with luminosity or with radius, i.e., a Tully-Fisher (1977) relation. The pairs of rotation curves in Figure 5 show that we do not observe such a correlation. Galaxies of the same HT and same $V_{\max}$ have radii which differ by factors of 2, and luminosities which differ by factors of 3.

V. CONCLUSIONS

The major result of this work is the observation that rotation curves of high-luminosity spiral galaxies are flat, at nuclear distances as great as $r = 50$ kpc. Roberts and his collaborators (Roberts 1976) deserve credit for first calling attention to flat rotation curves. Recent 21 cm observations by Krumm and Salpeter (1976, 1977) have strengthened this conclusion. These results take on added importance in conjunction with the suggestion of Einasto, Kaasik, and Saar (1974), and Ostriker, Peebles, and Yahil (1974) that galaxies contain massive halos extending to large r. Such models imply that the galaxy mass increases significantly with increasing r which in turn requires that rotational velocities remain high for large r. The observations presented here are thus a necessary but not sufficient condition for massive halos. As shown above, mass distributions from disk models or spherical models adequately reproduce the observed velocities. The choice between spherical and disk models is not constrained by these observations.

REFERENCES

Brandt, J. C. 1960, *Ap. J.*, **131**, 293.
Brosche, P. 1971, *Astr. Ap.*, **13**, 293.
Burbidge, E. M., and Burbidge, G. R. 1975, in *Galaxies and the Universe*, ed. A. and M. Sandage and J. Kristian (Chicago: University of Chicago Press).
de Vaucouleurs, G., de Vaucouleurs, A., and Corwin, H. G. 1976, *Second Reference Catalogue of Bright Galaxies* (Austin: University of Texas).
Einasto, J., Kaasik, A., and Saar, E. 1974, *Nature*, **250**, 309.
Holmberg, E. 1964, *Uppsala Astr. Obs. Medd.*, No. 148.
———. 1975, in *Galaxies and the Universe*, ed. A. and M. Sandage and J. Kristian (Chicago: University of Chicago Press).
Hubble, E. 1926, *Ap. J.*, **64**, 321.
Krumm, N., and Salpeter, E. E. 1976, *Ap. J. (Letters)*, **208**, L7.
———. 1977, *Astr. Ap.*, **56**, 465.
Kuz'min, G. G. 1952, *Pub. Tartu Astr. Obs.*, **32**, 211.
Nilson, P. 1973, *Uppsala Obs. Ann.*, Vol. **6**.
Ostriker, J. P., Peebles, P. J. E., and Yahil, A. 1974, *Ap. J. (Letters)*, **193**, L1.
Peterson, C. J., Rubin, V. C., Ford, W. K., Jr., and Roberts, M. S. 1978, *Ap. J.*, Vol. **226**, in press (Paper III).

Roberts, M. S. 1969, *A.J.*, **74**, 859.
———. 1975, in *Galaxies and the Universe*, ed. A. and M. Sandage and J. Kristian (Chicago: University of Chicago Press).
———. 1976, *Comments Ap.*, **6**, 105.
Rubin, V. C., Ford, W. K., Jr., Strom, K. S., Strom, S. E., and Romanishin, W. 1978, *Ap. J.*, **224**, 782 (Paper II).
Rubin, V. C., Thonnard, N., and Ford, W. K., Jr. 1977, *Ap. J. (Letters)*, **217**, L1 (Paper I).
Sandage, A. 1978, in preparation.
Sandage, A., Freeman, K. C., and Stokes, N. R. 1970, *Ap. J.*, **160**, 831.
Schweizer, F. 1978, *Ap. J.*, **220**, 98.
Shostak, S. 1978, *Astr. Ap.*, submitted.
Thonnard, N., Rubin, V. C., Ford, W. K., Jr., and Roberts, M. S. 1978, *A.J.*, submitted.
Tully, R. B., and Fisher, J. R. 1977, *Astr. Ap.*, **54**, 661.
Zwicky, F., Herzog, E., Wild, P., Karpowicz, M., and Kowal, C. T. 1961–1968, *Catalogue of Galaxies and Clusters of Galaxies* (Pasadena: California Institute of Technology), Vols. **1–6**.

W. KENT FORD, JR., VERA C. RUBIN, and NORBERT THONNARD: Department of Terrestrial Magnetism, Carnegie Institution of Washington, 5241 Broad Branch Road, N.W., Washington, DC 20015